Journal of the American College of Cardiology Vol. 59, No. 17, 2012

Published by Elsevier Inc.
ISSN 0735-1097/$36.00
doi:10.1016/j.jacc.2011.12.037

Cardiac Imaging

Coronary Arterial 18F-Sodium Fluoride Uptake

A Novel Marker of Plaque Biology

Marc R. Dweck, MD,*† Marcus W. L. Chow,*† Nikhil V. Joshi, MD,*† Michelle C. Williams, MD,*† Charlotte Jones, BSc,*† Alison M. Fletcher, PhD,† Hamish Richardson, BSc,† Audrey White,* Graham McKillop, MD,† Edwin J. R. van Beek, PhD,† Nicholas A. Boon, MD,* James H. F. Rudd, PhD,‡ David E. Newby, DSc*†

Edinburgh and Cambridge, United Kingdom

Objectives With combined positron emission tomography and computed tomography (CT), we investigated coronary arterial uptake of 18F-sodium fluoride (18F-NaF) and 18F-fluorodeoxyglucose (18F-FDG) as markers of active plaque calcification and inflammation, respectively.

Background The noninvasive assessment of coronary artery plaque biology would be a major advance particularly in the identification of vulnerable plaques, which are associated with specific pathological characteristics, including microcalcification and inflammation.

Methods We prospectively recruited 119 volunteers (72 ± 8 years of age, 68% men) with and without aortic valve disease and measured their coronary calcium score and 18F-NaF and 18F-FDG uptake. Patients with a calcium score of 0 were used as control subjects and compared with those with calcific atherosclerosis (calcium score >0).

Results Inter-observer repeatability of coronary 18F-NaF uptake measurements (maximum tissue/background ratio) was excellent (intra-class coefficient 0.99). Activity was higher in patients with coronary atherosclerosis (n = 106) versus control subjects (1.64 ± 0.49 vs. 1.23 ± 0.24; p = 0.003) and correlated with the calcium score (r = 0.652, p < 0.001), although 40% of those with scores >1,000 displayed normal uptake. Patients with increased coronary 18F-NaF activity (n = 40) had higher rates of prior cardiovascular events (p = 0.016) and angina (p = 0.023) and higher Framingham risk scores (p = 0.011). Quantification of coronary 18F-FDG uptake was hampered by myocardial activity and was not increased in patients with atherosclerosis versus control subjects (p = 0.498).

Conclusions 18F-NaF is a promising new approach for the assessment of coronary artery plaque biology. Prospective studies with clinical outcomes are now needed to assess whether coronary 18F-NaF uptake represents a novel marker of plaque vulnerability, recent plaque rupture, and future cardiovascular risk. (An Observational PET/CT Study Examining the Role of Active Valvular Calcification and Inflammation in Patients With Aortic Stenosis; NCT01358513) (J Am Coll Cardiol 2012;59:1539–48) © 2012 by the American College of Cardiology Foundation

Myocardial infarction (MI) is the foremost cause of death in developed countries (1) and confers a major economic, social, and healthcare burden worldwide (2). The majority of MIs result from rupture of atherosclerotic plaque, although identifying those at risk of rupture is problematic. The vast majority (86%) of culprit atherosclerotic lesions cause non-flow limiting luminal stenosis (3,4) that will not be detected by noninvasive stress testing. New methods focusing on plaque pathology are required to identify high-risk lesions so that risk of clinical events can be reduced by appropriate therapy.

See page 1549

Calcification is a key feature of human atherosclerosis, and its macroscopic presence in the coronary arteries can be detected by cardiac computed tomography (CT). Coronary

From the *Centre for Cardiovascular Sciences, University of Edinburgh, United Kingdom; †Clinical Research Imaging Centre, University of Edinburgh, Edinburgh, United Kingdom; and the ‡Division of Cardiovascular Medicine, University of Cambridge, Cambridge, United Kingdom. The Clinical Research Imaging Centre is supported by National Health Service Research Scotland through National Health Service Lothian. Dr. Dweck was supported by a fellowship grant from the British Heart Foundation (FS/10/026) and the British Heart Foundation Centre of Research Excellence Award. Dr. Joshi is supported by Chief Scientist Office (ETM/160). Dr. van Beek is supported by the Scottish Imaging Network—a Platform of Scientific Excellence. Dr. Williams has lectured at meetings sponsored by Toshiba. The work of Dr. Rudd is supported by HEFCE, the British Heart Foundation, and the Cambridge NIHR Biomedical Research Centre. Dr. Newby is supported by the British Heart Foundation (CH/09/002). All other authors have reported that they have no relationships relevant to the contents of this paper to disclose. Drs. Rudd and Newby contributed equally to this work and are joint senior authors.

Manuscript received October 12, 2011; revised manuscript received December 14, 2011, accepted December 20, 2011.

JACC Vol. 59, No. 17, 2012
April 24, 2012:1539–48

Abbreviations and Acronyms

18F-FDG = 18F-fluorodexyglucose
18F-NaF = 18F-sodium fluoride
CAC = coronary artery calcium
CAD = coronary artery disease
CHD = coronary heart disease
CI = confidence interval
CT = computed tomography
CVA = cerebrovascular accident
CVD = cardiovascular disease
LAD = left anterior descending coronary artery
MACE = major adverse cardiovascular events
MI = myocardial infarction
PET = positron emission tomography
SUV = standard uptake value
TBR = tissue/background ratio

artery calcium (CAC) scoring provides a surrogate measure of the atherosclerotic burden and a powerful predictor of cardiovascular risk (5). Risk prediction can be improved by examining the progression of coronary calcification (6,7) and by detecting spotty calcification (8). However, CT is unable to measure active calcification directly and cannot reliably detect micro-calcifications that can lead to microfractures and acute thrombosis (9–11). 18F-sodium fluoride (18F-NaF) is an established positron emission tomography (PET) tracer that detects novel areas of bone formation and remodeling (12). Uptake has also been described in aortic and carotid atheroma where activity is believed to signal areas of active vascular calcification, although this is hypothetical (13–15). To date, 18F-NaF uptake has not been measured in the coronary vasculature.

Inflammation is thought to play a key role in plaque rupture. Histologically, the vulnerable plaque is characterized by a lipid-rich pool, infiltration of inflammatory cells, and a thin fibrous cap (4). Macrophages in particular are found in abundance within ruptured plaques and are thought to contribute to a pro-thrombotic state and degradation of the fibrous cap via the action of matrix metalloproteinases (16). Vascular inflammation can be assessed noninvasively in the carotid arteries, aorta, iliac, and femoral arteries with uptake of 18F-fluorodeoxyglucose (18F-FDG) as measured by combined PET and computed tomography (CT) (17). 18F-FDG uptake correlates with plaque macrophage burden (18), symptoms (19), and Framingham Risk Score (20) and can be lowered with statin and other therapies (21,22). Recent in vitro and ex vivo data have also suggested that 18F-FDG uptake might reflect plaque hypoxia (23). However, measurement of 18F-FDG uptake within coronary atheroma is challenging, because of cardiac and respiratory motion and the intense myocardial 18F-FDG uptake that can potentially swamp any plaque signal (24,25).

The aim of this study was to investigate coronary arterial uptake of 18F-NaF and 18F-FDG as markers of active calcification and inflammation, respectively. We hypothesized that the degree of uptake of both tracers would correlate with atherosclerotic disease severity, symptoms, prior cardiovascular events, and predictors of future clinical risk.

Methods

Study population. This was a substudy of a previously published prospective cohort of 121 apparently healthy volunteers and patients with aortic sclerosis and stenosis (26). All subjects were over 50 years of age and consecutively recruited from cardiology outpatient clinics (Royal Infirmary Edinburgh) to achieve groups of similar age and sex. Exclusion criteria included insulin-dependent diabetes mellitus, poorly controlled type 2 diabetes mellitus, women of childbearing potential not taking contraception, inability to undergo PET/CT scanning, and life expectancy <2 years. The study was approved by the local research ethics committee, and written informed consent was obtained from all subjects.

Baseline clinical assessment. Baseline clinical assessment was performed on the day of the initial PET/CT scan and included current cardiac symptoms, prior coronary intervention (percutaneous coronary intervention and coronary artery bypass grafting), and past medical history of previous major adverse cardiovascular events (MACE) (MI, cerebrovascular accident, and coronary revascularization). Atherogenic risk factors such as age, sex, smoking habit, history of hypertension, diabetes mellitus, hypercholesterolemia, socioeconomic status, and family history of cardiovascular disease were identified. Full external examination was performed, and height and weight were measured to determine body mass index. A 12-lead electrocardiogram was performed, and venous blood was collected for measurement of serum creatinine, full lipid profile, and markers of calcium metabolism. On the basis of this information, Framingham risk scores for coronary heart disease (CHD), CHD death, cardiovascular disease (CVD), and CVD death were calculated.

Dietary restrictions. Myocardial uptake of 18F-FDG can cause overspill of signal into the coronary arteries, leading to difficulties in discriminating coronary artery uptake from myocardium. All patients in our cohort were asked to observe a carbohydrate-free, high-fat diet for 24 h before their 18F-FDG scan. This suppresses myocardial uptake by switching the heart from glucose to free-fatty acid metabolism (27–29). Patients were provided with written instructions and contacted by phone the day before the scan in an attempt to ensure dietary compliance.

PET/CT image acquisition and reconstruction. Subjects underwent combined PET/CT imaging of the aorta and coronary arteries with a hybrid scanner (Biograph mCT, Siemens Medical Systems, Erlangen, Germany). For the first scan, an electrocardiogram-gated breath-hold CT scan (non-contrast-enhanced, 40 mAs/rot [CareDose, Siemens Medical Systems], 100 kV) of the coronary arteries was performed for calculation of the CAC score. Study subjects were then administered a target dose of 125 MBq 18F-NaF intravenously and subsequently rested in a quiet environment for 60 min. An attenuation correction CT scan (non-enhanced 120 kV and 50 mA) was then performed, followed by PET imaging of the thorax in 3-dimensional mode for 10 min.

For the second scan, subjects were administered a target dose of 200 MBq 18F-FDG intravenously and subsequently rested in a quiet environment for 90 min. Combined PET/CT imaging was then performed as described for the 18F-NaF scan but with a 15-min bed time. Tracer circulation times were based on previous studies with 18F-FDG and 18F-NaF in atherosclerosis and aimed for optimal contrast between the aortic wall, coronary arteries, and the blood pool (14,15,19). The PET data were reconstructed with the Siemens Ultra-HD (time of flight +True X) reconstruction algorithm. Corrections were applied for attenuation, dead time, scatter, and random coincidences. All image analysis was performed on fused PET/CT datasets.

Image analysis: coronary arteries. Evaluation of the calcium score was performed with calcium score analysis software (VScore, Vital Images, Minnetonka, Minnesota). Vessel-specific and total Agatston calcium scores were calculated as described previously (30). The PET and CT images were fused and analyzed by an experienced reader with an Osirix workstation (OsiriX version 3.5.1 64-bit; OsiriX Imaging Software, Geneva, Switzerland). For 18F-NaF uptake, the coronary arteries were visually identified, and regions of interest were drawn around areas of maximal uptake in the left main stem, left anterior descending artery, circumflex artery, and the right coronary artery. The maximum standard uptake value (SUV) was recorded from these regions. It was not possible to determine the mean SUV values, given the difficulty in identifying the exact borders of the coronary arteries on the non-contrast-enhanced scans. The SUV is the decay-corrected tissue concentration of 18F-NaF divided by the injected dose/body weight. However, SUV measurements in vascular structures are influenced by variability in 18F-FDG and 18F-NaF activity in the blood. Therefore, SUV measurements were divided by an averaged mean SUV value in the blood pool, derived from 5 circular regions of interest drawn in the center of the superior vena cava. This provided maximum tissue/background ratios (TBRs) as a measure of arterial tracer uptake (18,31).

Quantification of 18F-FDG uptake was performed as for 18F-NaF but restricted to the proximal and mid-portions of the coronary vessels (24). Difficulties were still encountered as a result of the pervasive myocardial uptake observed with this tracer, and coronary activity was only quantified in areas where myocardial uptake could be confidently avoided.

INTER-OBSERVER REPEATABILITY OF IMAGE ANALYSIS. After the image analysis methodology was established, PET scans from 20 patients were selected at random from the cohort. All scans from these patients were analyzed independently by 2 trained observers (M.D., N.J.). This provided measures of inter-observer repeatability for maximum TBR values.

Image analysis: aorta. The uptake of 18F-FDG (32) and 18F-NaF (13) in the ascending and descending aorta was quantified as per published methods. Circular regions of interest were drawn around the aorta on adjacent 3-mm axial slices with care taken to avoid uptake from extravascular structures. Maximum SUV values were once more corrected for blood-pool activity to provide TBR values.

Statistical analysis. Comparisons of tracer uptake were initially made between those with and without calcific atherosclerosis. Patients with CAC scores >0 or a prior history of ischemic heart disease were considered to have underlying calcific coronary atherosclerosis. Patients with a CAC score of 0 and no past history of CHD were considered not to have calcific atherosclerosis and designated as control subjects. Patients with atherosclerosis were then divided according to well-established cutoffs in the coronary calcium score (0, 1 to 100, 101 to 400, 401 to 1,000, >1,000) (33) to assess the impact of disease severity on tracer activity. Finally, comparisons were made between subjects who had normal and increased 18F-NaF uptake. The highest maximum TBR value in the control group was used as the cutoff value above which 18F-NaF was deemed to be elevated. In patients with underlying calcific coronary atherosclerosis, those who had increased 18F-NaF uptake were defined as having active coronary calcification, whereas those with normal 18F-NaF uptake were defined as having inactive calcification.

Continuous variables were expressed as mean ± SD and compared with unpaired Student *t* test or 1-way analysis of variance where appropriate. Categorical variables were expressed as percentages and analyzed with the chi-square test. Correlations between normally distributed data were performed with Pearson's correlation, whereas Spearman's correlation was used for nonparametric data. The 95% normal range for differences between sets of SUV and TBR measurements (the limits of agreement) were estimated by multiplying the SD of the mean difference by 1.96 (34). Intra-class correlation coefficients with 95% confidence intervals (CIs) were calculated for intraobserver and interobserver variation. Statistical analysis was performed with SPSS software (version 18, SPSS, Inc., Chicago, Illinois). A 2-sided p value <0.05 was regarded as statistically significant.

Results

Baseline characteristics. A total of 119 patients were recruited (age 72 ± 8 years, 68% men, 66% with aortic stenosis) and had both 18F-NaF (66 ± 6 min after 124 ± 10 MBq) and 18F-FDG (94 ± 7 min after 198 ± 13 MBq) scans of their thorax <1 month apart (median 7 days, interquartile range 1 to 14 days). The effective radiation dose/patient, including all PET and CT scans, was 9.73 ± 1.19 mSv with a CT conversion factor of 0.014 mSv/mGy/cm.

Thirteen patients had no past history of coronary artery disease (CAD) or evidence of calcific coronary atherosclerosis and formed the control group (Table 1). A total of 106 patients had evidence of coronary atherosclerosis: 41 having a clinical diagnosis of prior CAD, and a further 65 having calcium scores above 0. One patient had experienced an

JACC Vol. 59, No. 17, 2012
April 24, 2012:1539–48

Table 1 Patient Demographic Data

			Atherosclerosis			
	Total	Control Ca Score 0	Ca Score 1–100	Ca Score 101–400	Ca Score 401–1,000	Ca Score >1,000
n	119	13	19	23	27	37
Age (yrs)	72 ± 8	66 ± 7	69 ± 8	72 ± 8	70 ± 9	76 ± 7
Male, %	68	46	58	61	74	81
BMI, kg/m^2	28 ± 4	28 ± 4	28 ± 3	28 ± 4	28 ± 4	27 ± 5
CHD, %	34	0	0	17	48	65
Angina, %	24	0	0	13	37	43
MACE, %	40	0	0	32	44	75
Previous MI	12	0	0	9	11	24
Previous CVA/TIA	6	0	0	14	4	8
Previous PCI	15	0	0	9	22	27
Previous CABG	7	0	0	0	7	16
Smokers (ex or current), %	50	38	53	26	59	59
Diabetes, %	15	23	5	13	12	22
Hypertension, %	60	38	42	65	52	57
Hypercholesterolemia, %	49	38	39	39	59	57
Aortic stenosis, %	66	54	58	61	78	73
Aortic sclerosis, %	17	23	11	22	11	19
ACEi/ARB, %	49	15	21	39	56	76
Beta-blockers, %	39	15	26	48	44	46
Statins, %	53	15	21	52	67	73
Total cholesterol, mg/dl	193 ± 50	227 ± 48	199 ± 41	204 ± 57	175 ± 44	181 ± 49
LDL cholesterol, mg/dl	104 ± 44	123 ± 45	119 ± 37	112 ± 52	93 ± 36	94 ± 42
HDL cholesterol, mg/dl	54 ± 20	69 ± 42	54 ± 12	52 ± 15	54 ± 18	51 ± 12
Creatinine, mg/dl	0.98 ± 0.33	0.97 ± 0.12	0.90 ± 0.13	0.93 ± 0.12	0.88 ± 0.14	0.86 ± 0.12
Calcium, mg/dl	9.30 ± 0.57	9.41 ± 0.23	9.41 ± 0.97	9.29 ± 0.61	9.24 ± 0.32	9.24 ± 0.49
Phosphate, mg/dl	3.55 ± 0.49	3.68 ± 0.55	3.57 ± 0.55	3.51 ± 0.40	3.53 ± 0.40	3.54 ± 0.48
Alk Phosphatase, U/l	84 ± 44	93 ± 23	83 ± 25	79 ± 20	80 ± 23	77 ± 27
Ca score	414 (79–1,251)	0 (0–0)	19 (2–46)	277 (125–351)	734 (448–888)	1783 (1,357–3,410)
18F-NaF Max SUV	1.56 ± 0.50	1.21 ± 0.26	1.28 ± 0.27	1.40 ± 0.27	1.49 ± 0.31	1.97 ± 0.60
18F-NaF Max TBR	1.59 ± 0.48	1.23 ± 0.22	1.33 ± 0.32	1.42 ± 0.27	1.59 ± 0.29	1.97 ± 0.58
Patients with increased coronary 18F-NaF, %	34%	0%	5%	26%	41%	59%
18F-FDG Max SUV	1.54 ± 0.24	1.43 ± 0.30	1.56 ± 0.19	1.55 ± 0.27	1.46 ± 0.24	1.60 ± 0.22
18F-FDG Max TBR	1.22 ± 0.21	1.18 ± 0.31	1.25 ± 0.18	1.19 ± 0.16	1.22 ± 0.29	1.24 ± 0.15
10-yr Framingham risk scores						
CVD	30 ± 13	25 ± 17	27 ± 13	31 ± 10	27 ± 12	35 ± 13
CVD death	14 ± 10	8 ± 9	11 ± 8	14 ± 8	12 ± 10	18 ± 11
CHD	19 ± 12	16 ± 15	18 ± 11	20 ± 10	18 ± 12	22 ± 12
CHD death	6.3 ± 4.7	4.5 ± 5.4	5.2 ± 3.9	6.3 ± 3.6	5.3 ± 4.4	8.3 ± 5.1

Values are mean ± SD, %, or median (interquartile range). 18F-NaF and 18-FDG values are based upon the maximum values recorded in the coronary vasculature of each patient.

18F-FDG = 18F-fluorodexyglucose; 18F-NaF = 18F-sodium fluoride; ACEi = angiotensin-converting enzyme inhibitors; Alk = alkaline; ARB = angiotensin receptor blocker; BMI = body mass index; Ca score = Agatston coronary calcium score; CABG = coronary artery bypass graft; CHD = coronary heart disease; CVA = cerebrovascular accident; CVD = cardiovascular disease; HDL = high-density lipoprotein; LDL = low-density lipoprotein; MACE = major adverse cardiovascular events; MI = myocardial infarction; PCI = percutaneous coronary intervention; SUV = standard uptake value; TBR = tissue/background ratio; TIA = transient ischemic attack.

acute coronary syndrome in the week before his 18F-NaF scan; otherwise, patients had stable CHD.

Dietary restrictions. Average myocardial SUV across the entire cohort was 4.6 ± 3.6, and dietary restrictions effectively suppressed 18F-FDG myocardial uptake (prespecified as a maximum SUV <5 measured in the maximal area of uptake in the left ventricular septum) in 67% of patients, similar to that seen in previous studies (24). Sixty-one percent of patients complied with the dietary restrictions, on the basis of dietary diaries, and had lower myocardial 18F-FDG uptake than non-compliers (SUV 3.2 ± 2.3 vs. 6.7 ± 4.2; $p < 0.001$).

18F-NaF coronary uptake. Coronary 18F-NaF uptake was quantifiable in 96% of the coronary territories examined. It was not possible to assess the left main stem in 20 patients, due to overspill of activity from the aortic valve secondary to calcific aortic stenosis (Table 2). Repeatability studies were excellent for coronary 18F-NaF quantification with no fixed or proportional biases, limits of agreement of ±0.14 for maximum TBR values (Fig. 1), and an intra-class

Table 2 18F-NaF and 18F-FDG SUV Max and TBR Max Values

	Coronary Arteries						
	LMS	LAD	CX	RCA	All Vessels	Ascending Aorta	Descending Aorta
18F-NaF							
% interpretable	83%	100%	99%	100%	96%	100%	100%
SUV max	1.36 ± 0.40	1.32 ± 0.46	1.38 ± 0.42	1.27 ± 0.41	1.56 ± 0.50	1.97 ± 0.43	2.01 ± 0.40
TBR max	1.36 ± 0.44	1.35 ± 0.46	1.42 ± 0.42	1.30 ± 0.41	1.59 ± 0.48	2.01 ± 0.31	2.06 ± 0.35
% with increased activity (TBR >1.61)	13%	21%	19%	16%	34%	—	—
Interobserver limits of agreement (mean difference ± 2 SD)	0.06 ± 0.17	0.01 ± 0.20	0.00 ± 0.21	0.01 ± 0.21	0.03 ± 0.14	—	—
18F-FDG							
% interpretable	25%	74%	33%	74%	51%	100%	100%
SUV max	1.55 ± 0.25	1.45 ± 0.27	1.48 ± 0.28	1.34 ± 0.22	1.54 ± 0.24	2.23 ± 0.35	2.24 ± 0.31
TBR max	1.20 ± 0.23	1.14 ± 0.23	1.14 ± 0.19	1.05 ± 0.24	1.22 ± 0.21	1.78 ± 0.25	1.79 ± 0.25
Interobserver limits of agreement	−0.09 ± 0.28	−0.21 ± 0.48	−0.12 ± 0.42	−0.23 ± 0.30	−0.22 ± 0.32	—	—

The 18F-NaF and 18F-FDG maximum standard uptake values (SUV max) and tissue/background ratio (TBR max) values in the coronary arteries, ascending aorta, and descending aorta. Inter-observer repeatability statistics are also provided for TBR maximum measurements in each of the coronary territories (mean difference ± limits of agreement).

CX = circumflex; LAD = left anterior descending coronary artery; LMS = left main stem; RCA = right coronary artery; other abbreviations as in Table 1.

correlation coefficient value of 0.99 (95% CI: 0.98 to 1.00). Limits of agreement for 18F-NaF were in the order ±0.20 when examined in each of the coronary territories (Table 2).

18F-NaF activity was observed in areas overlying, adjacent to, and remote from existing coronary calcification. Uptake was focal in nature and could be localized to individual coronary plaques. Areas of coronary calcification with no 18F-NaF uptake were also commonly observed (Fig. 2).

Coronary 18F-NaF uptake was higher in those with coronary atherosclerosis, compared with the control group (1.64 ± 0.49 vs. 1.23 ± 0.24; p = 0.003) (Table 1). The highest maximum TBR value in the control group was 1.61, which was used to divide patients with coronary atherosclerosis into those with increased 18F-NaF uptake (active calcification; TBR maximum >1.61; n = 40) and those without (inactive calcification; TBR maximum ≤1.61; n = 66) (Fig. 2, Table 3).

Patients with increased 18F-NaF uptake were older, more likely to be male, and had lower serum high-density lipoprotein cholesterol concentrations than those without increased uptake (Table 3). Overall statin use was similar between the groups, although atorvastatin use seemed to be double in those with active calcification (28% vs. 14%; p = 0.077). They also had higher calcium scores, and there was a strong correlation between the CAC score and 18F-NaF uptake (r = 0.652, p < 0.001). However extensive overlap was observed, with some patients with increased 18F-NaF uptake having relatively little coronary calcification (minimum Agatston score 98) and patients without 18F-NaF uptake having extensive calcium (maximum Agatston score 4,636). Indeed 41% of patients with CAC scores >1,000 had no significant 18F-NaF uptake (Table 1).

Sites of increased 18F-NaF uptake were evenly distributed across the coronary vasculature (Table 2), and activity was 50% higher on average in these plaques compared with inactive plaques in the same patient (2.14 ± 0.42 vs. 1.43 ± 0.32; p < 0.001). In 25 patients, significant uptake was observed in 2 or more coronary territories.

Patients with high 18F-NaF uptake were more likely to have a clinical diagnosis of CAD (60% vs. 26%; p < 0.001), anginal symptoms (40% vs. 20%; p = 0.023), prior revascularization (38% vs. 11%: p = 0.001), and previous MACE (45% vs. 23%; p < 0.016) (Table 3). Furthermore, cardiovascular risk factor burden was increased. Framingham risk prediction scores were higher in those with increased 18F-NaF uptake in terms of Framingham CVD (p = 0.033), CHD (p = 0.049), CVD death (p = 0.011), and CHD death (p = 0.024) (Fig. 3, Table 3). Interestingly 10-year Framingham risk scores for CVD, CVD death, and CHD death all displayed a correlation with 18F-NaF coronary uptake but not with the CAC score (Table 4). Framingham risk scores are not designed for patients with prior cardiovascular events. If these patients were excluded from the analysis, risk scores remained higher in those with active calcification for both CHD (18 ± 12 vs. 26 ± 12; p = 0.020) and CVD (29 ± 13 vs. 37 ± 12; p = 0.017).

One patient was assessed 1 week after sustaining an inferior non–ST-segment elevation MI. Intense uptake was observed in the proximal right coronary artery, which had been felt clinically to be the culprit coronary artery (on the basis of dynamic changes on the electrocardiogram and appearances at invasive coronary angiography). Relatively little uptake was observed in his other coronary territories, despite having 3-vessel CAD and extensive coronary calcification (Fig. 2, Online Video).

18F-FDG coronary uptake. The 18F-FDG uptake was difficult to quantify, particularly in the left main stem and circumflex artery. It was not possible to quantify accurately in 49% of the vessel territories examined (Table 2). This was largely the result of myocardial spill over into the coronary arteries, which was observed despite the dietary restrictions imposed in the study. Even when possible, coronary 18F-FDG repeatability was inferior to that for 18F-NaF, with a

JACC Vol. 59, No. 17, 2012
April 24, 2012:1539–48

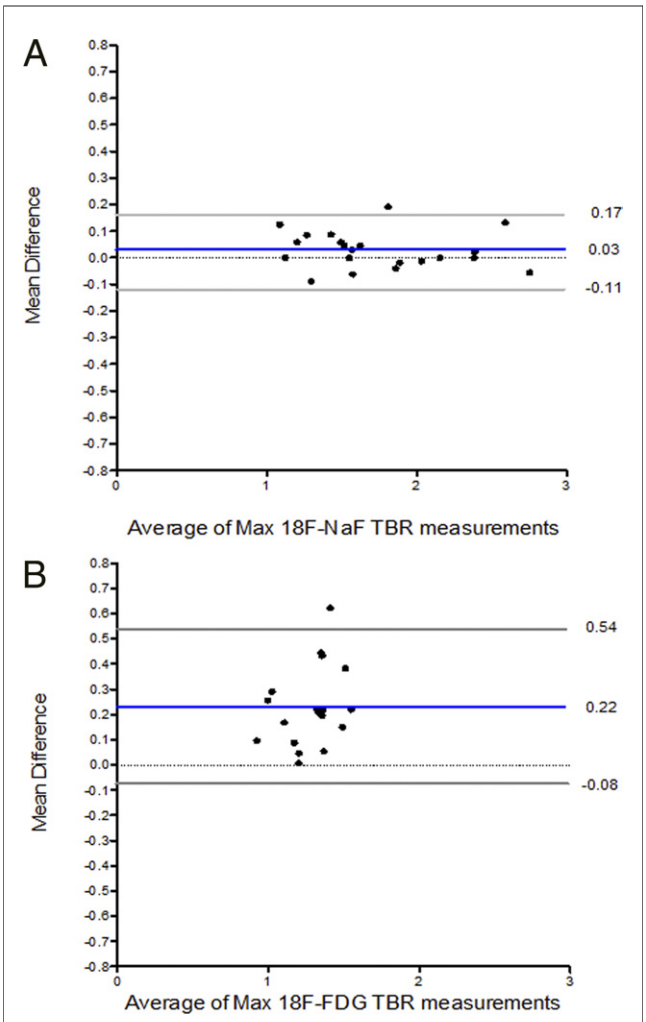

Figure 1 **Bland Altman Plot of Inter-Observer Repeatability for Max TBR Values for 18F-NaF and 18F-FDG**

Bland Altman plot of inter-observer repeatability for maximum (Max) tissue/background ratio (TBR) values for **(A)** 18F-sodium fluoride (18F-NaF) and **(B)** 18F-fluorodeoxyglucose (18F-FDG). **Blue line** shows the mean inter-observer difference. **Grey lines** show the limits of agreement for measurements.

fixed bias of 0.22, limits of agreement of ± 0.32 and an intra-class correlation coefficient value of 0.67 (95% CI: 0.31 to 0.86) (Fig. 1).

There were no differences in 18F-FDG uptake between the control group and those with atherosclerosis (1.18 ± 0.31 vs. 1.23 ± 0.20; p = 0.498) (Table 1). There also was no correlation between 18F-FDG activity and the CAC score, whether in the coronary vasculature as a whole (r = 0.063, p = 0.538) or on a vessel-by-vessel basis (LAD: r = −0.041, p = 0.705; RCA: r = 0.039, p = 0.726). The 18F-FDG coronary uptake was not associated with increased rates of CAD, anginal symptoms, prior coronary revascularization, or previous MACE. Neither was there a significant correlation with any of the risk prediction scores (Table 4).

Aortic uptake. 18F-NaF uptake in the aorta was observed in a focal distribution most commonly in areas overlying or adjacent to existing aortic calcification (Fig. 4). Less frequently 18F-NaF uptake occurred in the absence of local calcium (Fig. 4, Table 2). Across the cohort as a whole, 18F-NaF uptake in the aorta was higher than in the coronary arteries (2.01 ± 0.31 vs. 1.59 ± 0.48; p < 0.001) (Table 2). Uptake in the ascending aorta correlated with activity in the descending aorta (r = 0.815, p < 0.001) and the coronary arteries (r = 0.525, p < 0.001) and with Framingham risk scores (e.g., ascending aorta vs. CVD: r = 0.208, p = 0.024). However, among those with increased coronary 18F-NaF activity, a correlation was no longer observed between activity in the coronary vasculature and the aorta (r = 0.157, p = 0.333).

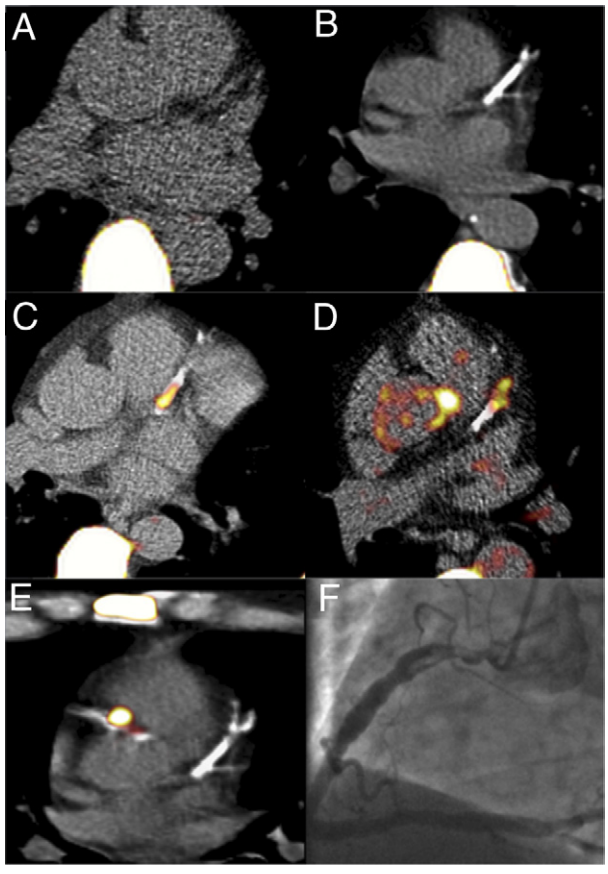

Figure 2 **Fused Positron Emission Tomography/Computed Tomography Images of 18F-NaF Activity in the Coronary Arteries**

(A) Patient in the control group with no coronary calcium and no coronary 18F-sodium fluoride (18F-NaF) uptake. Note the intense uptake in the vertebrae. **(B)** Patient with extensive calcification in the left anterior descending artery (LAD) but no 18F-NaF uptake. **(C)** Intense focal 18F-NaF uptake is observed in the proximal LAD overlying existing coronary calcium in this region. **(D)** Increased and focal 18F-NaF uptake is observed in the mid-LAD adjacent to an area of existing coronary calcification. **(E)** Patient who suffered a recent inferior non-ST-segment elevation myocardial infarction showing intense focal uptake of the proximal right coronary artery with sparing of the LAD. The proximal right coronary artery was felt to be the culprit artery on the basis of the electrocardiogram and appearances on coronary angiography **(F),** which demonstrated a complex ulcerated plaque with in situ thrombus (Online Video).

Table 3 Baseline Characteristics and 10-Year Framingham Risk Scores

	Low 18F-NaF Uptake (n = 66)	High 18F-NaF Uptake (n = 40)	p Value
Age, yrs	71 ± 8	75 ± 8	0.015*
Male, %	65	80	0.103
BMI, kg/m^2	27 ± 4	28 ± 5	0.343
CHD, %	26	60	<0.001†
Angina, %	20	40	0.023*
MACE, %	23	45	0.016*
Previous MI	11	18	0.324
Previous CVA/TIA	8	5	0.591
Previous PCI	9	30	0.005†
Previous CABG	2	18	0.003†
Smokers (ex/current), %	50	52	0.803
Diabetes, %	12	18	0.410
Hypertension, %	59	68	0.387
Hypercholesterolemia, %	49	53	0.745
ACEi/ARB, %	50	58	0.453
Beta-blockers, %	38	50	0.221
Statin, %	52	68	0.107
Atorvastatin, %	14	28	0.077
Total cholesterol, mg/dl	196 ± 48	174 ± 48	0.023*
LDL cholesterol, mg/dl	105 ± 43	96 ± 43	0.288
HDL cholesterol, mg/dl	55 ± 15	48 ± 11	0.021*
Creatinine, mg/dl	0.90 ± 0.14	0.87 ± 0.11	0.278
Calcium, mg/dl	9.21 ± 0.43	9.39 ± 0.79	0.125
Phosphate, mg/dl	3.55 ± 0.52	3.51 ± 0.43	0.647
Alkaline phosphatase, U/l	81 ± 23	87 ± 69	0.473
Coronary calcium score	372 (75–994)	1249 (589–2790)	<0.001†
Coronary 18F-NaF TBR max	1.34 ± 0.17	2.14 ± 0.42	<0.001†
Coronary 18F-FDG TBR max	1.23 ± 0.20	1.23 ± 0.20	0.875
10-yr Framingham risk scores			
CVD	29 ± 13	34 ± 12	0.033*
CVD death	12 ± 9	17 ± 11	0.011*
CHD	18 ± 11	23 ± 12	0.049
CHD death	5.8 ± 4.4	7.9 ± 4.6	0.024*

Values are mean ± SD, %, or median (interquartile range). Baseline characteristics and 10-year Framingham risk scores of patients with coronary atherosclerosis and either normal (SUV ≤1.61) or high (SUV >1.61) coronary 18F-NaF uptake. *p < 0.05 †p < 0.01
Abbreviations as in Table 1.

18F-FDG uptake was observed in a circumferential pattern around the aortic wall as previously described (Fig. 4) (17). Maximum 18F-FDG TBR in the ascending aorta correlated strongly with that in the descending aorta ($r = 0.824$, $p < 0.001$) and the coronary arteries ($r = 0.543$, $p < 0.001$). 18F-FDG activity was higher in the aorta than the coronary arteries (1.78 ± 0.25 vs. 1.22 ± 0.21; $p < 0.001$) (Table 2). There was no correlation between 18F-NaF and 18F-FDG uptake in the ascending aorta ($r = 0.043$, $p = 0.647$), descending aorta ($r = 0.124$, $p = 0.183$), or the coronary arteries ($r = 0.127$, $p = 0.21$).

Discussion

This is the first study to describe 18F-NaF uptake in the coronary arteries with PET/CT. We have demonstrated that this technique is both feasible and repeatable and that it can provide key insights into coronary artery plaque biology. Activity was higher in patients with atherosclerosis compared with control subjects, displaying a progressive rise with increasing atherosclerotic burden. Furthermore, 18F-NaF uptake can be used to discriminate between those patients with active and inactive coronary calcification. Those with active calcification (38%) were more likely to have clinically significant CAD, a higher incidence of previous MACE, lower serum high-density lipoprotein cholesterol concentrations, and higher Framingham risk prediction scores. Therefore, 18F-NaF holds promise as a means of identifying high-risk populations and refining the predictive power of CAC scoring. Finally, the spatial resolution of PET/CT allows localization of the 18-NaF signal to specific coronary territories and plaques offering the possibility of identifying vulnerable or culprit plaque on an individual basis.

18F-NaF uptake has been described recently in the aorta (14) and carotid arteries (15) and is believed to reflect active vascular calcification. Although histological validation of this hypothesis is lacking, mechanistic information can be extrapolated from 18F-NaF uptake in bone that has been studied for over 30 years. In that tissue, 18F-NaF is incorporated directly into exposed hydroxyapatite crystal via an exchange mechanism with hydroxyl groups (35). Therefore it detects novel areas of calcification as well as regions of remodeling and is used clinically in Paget's disease (36), primary osteoblastic tumors, and metastatic bone disease (37). Similarly, we believe that coronary uptake reflects active calcification in atherosclerotic plaque. Certainly coronary 18F-NaF uptake seems to offer information that is additional and complementary to CAC scoring. Although 18F-NaF activity was most commonly observed overlying

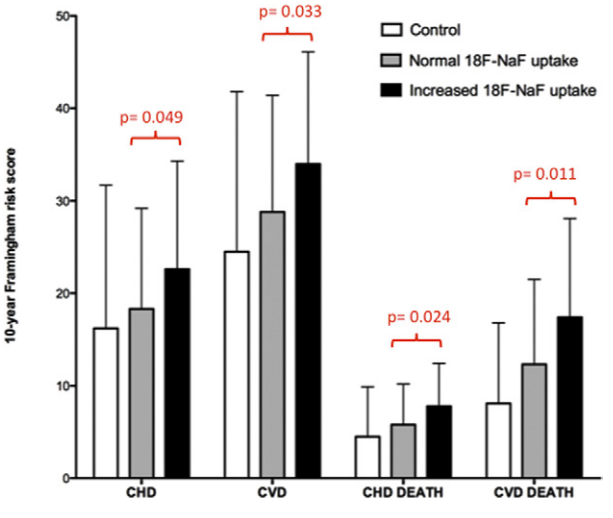

Figure 3 10-Year Framingham Risk Scores for Control Subjects and Patients With Atherosclerosis Who Did and Did Not Have Increased 18F-NaF Uptake

Error bars denote the SD of the mean. 18F-NaF = 18F-sodium fluoride; CHD = coronary heart disease; CVD = cardiovascular disease.

JACC Vol. 59, No. 17, 2012
April 24, 2012:1539–48

Table 4 Correlation of 10-Year Framingham Risk Scores With the Coronary Calcium Score and PET Uptake

	10-Yr Framingham Risk Scores			
	CVD Events	CVD Death	CHD Events	CHD Death
Coronary calcium score	r = 0.112	r = 0.152	r = 0.047	r = 0.110
	p = 0.230	p = 0.101	p = 0.617	p = 0.237
18F-NaF max TBR				
Coronary arteries	r = 0.196	r = 0.282	r = 0.138,	r = 0.220
	p = 0.035*	p = 0.002†	p = 0.137	p = 0.017*
Ascending aorta	r = 0.208	r = 0.239	r = 0.141	r = 0.195
	p = 0.024*	p = 0.009†	p = 0.129	p = 0.035*
Descending aorta	r = 0.199	r = 0.231	r = 0.144	r = 0.191
	p = 0.032*	p = 0.012*	p = 0.122	p = 0.039*
18F-FDG max TBR				
Coronary arteries	r = −0.024	r = 0.118	r = 0.059	r = 0.060
	p = 0.815	p = 0.245	p = 0.565	p = 0.560
Ascending aorta	r = −0.018	r = −0.047	r = 0.031	r = 0.012
	p = 0.845	p = 0.618	p = 0.741	p = 0.899
Descending aorta	r = −0.043	r = −0.052	r = 0.030	r = −0.019
	p = 0.645	p = 0.584	p = 0.752	p = 0.842

Correlation of 10-year Framingham risk scores with the coronary calcium score and 18F-NaF or 18F-FDG uptake in the coronary arteries and aorta.
*$p < 0.05$; †$p < 0.01$.
Abbreviations as in Table 1.

existing calcium and a strong correlation was observed with the CAC score, 41% of patients with scores >1,000 had no significant 18F-NaF uptake and, areas of increased tracer uptake were also found in regions remote from established calcium. This activity potentially relates to developing micro-calcification that is frequently beyond the resolution of CT and believed to be associated with increased mechanical stress and risk of future cardiovascular events (9–11). Therefore, 18F-NaF seems to distinguish between patients with dormant calcific disease, established many months or years previously, and subjects with metabolically active disease where the calcification process is ongoing. Importantly this distinction seems to be of clinical relevance, with higher rates of anginal symptoms, prior MACE events, and cardiovascular risk factor scores observed in those with active disease.

Calcification plays a key role in the pathophysiology of atherosclerosis, although its triggers remain debated. Atherosclerotic plaques with healed rupture almost invariably contain calcium (38,39), leading to the hypothesis that calcification forms part of a healing response to such events (7,40,41). The spatial resolution of PET/CT is sufficient to localize 18F-NaF activity to specific coronary territories, suggesting that 18F-NaF might be able to identify the presence and location of recent plaque rupture. This is supported by the PET/CT findings in the patient with recent MI. Extensive calcification was present in all 3 vessels, yet increased 18F-NaF was only observed in the culprit lesion, which was found to be complex and associated with thrombus at the time of coronary angiography. According to this hypothesis, the increased 18F-NaF activity observed in patients with stable CAD reflects sub-clinical plaque rupture that has been demonstrated in over 10% of such patients undergoing angioscopy (42,43) and is thought to underlie the step-wise growth of coronary atheroma.

Coronary calcification might occur as a response to intense plaque inflammation. Similar calcific responses can be observed in other inflammatory conditions such as tuberculosis, and intra-vascular ultrasound studies have recently associated micro-calcification with a large necrotic core (44). However, this theory is not supported by our 18F-FDG data, which failed to show a correlation with 18F-NaF activity in either the coronary arteries or the aorta, indicating that inflammation and calcification occur independently in these regions.

By contrast to 18F-NaF, 18F-FDG activity was not increased in patients with coronary atherosclerosis, compared with control subjects. However, our data were hampered by myocardial uptake that rendered one-half of the coronary territories un-interpretable. This largely reflected the imperfect dietary compliance that occurred in one-third of patients, despite the detailed written instructions and verbal reminders provided. Further studies are required in younger cohorts in whom compliance might be improved, although our data do suggest that 18F-FDG might be of limited use in the assessment of stable coronary disease. Inflammation has a more prominent role in acute coronary syndromes, and therefore 18-FDG might provide more information in these patients. Indeed a recent study demonstrated increased 18F-FDG uptake in unstable versus stable plaque in the proximal coronary vasculature (24).

Study limitations. Positron emission tomography/CT is expensive, especially when compared with circulating biomarkers of calcification activity, and this might limit its clinical use.

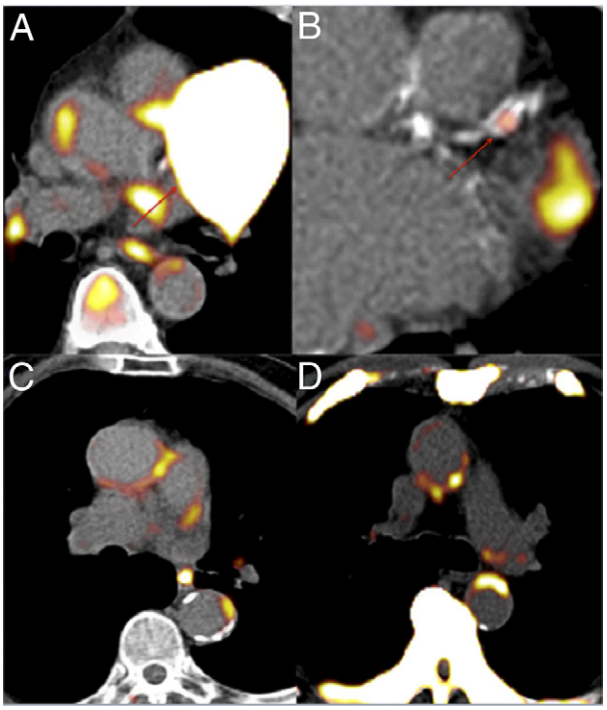

Figure 4 **Vascular Positron Emission Tomography/Computed Tomography Scans in the Coronary Arteries and Aorta**

(A) 18F-FDG. Intense 18F-FDG myocardial uptake is observed that obscures uptake in the coronary arteries, although activity can be observed in the descending aorta. **(B)** Effective myocardial suppression has been achieved, and a focal area of uptake can be observed in the mid-LAD. **(C)** Increased 18F-FDG activity can be observed in a circumferential pattern in both the ascending and descending aortae that rarely overlapped with existing aortic calcium. **(D)** 18F-NaF. Increased 18F-NaF uptake is present in the ascending and descending aortae remote from existing vascular calcification. Also note activity in in the ribs, sternum, and vertebra. Abbreviations as in Figures 1 and 2.

However, we have demonstrated that—among those with increased 18F-NaF uptake—activity in the coronaries did not correlate with that in the aorta, suggesting that it is driven by local rather than systemic factors. Therefore blood-based biomarkers are unlikely to provide an accurate indication of coronary calcification activity and instead will tend to reflect that within larger vessels or skeletal bone. Therefore, in our opinion the added costs of PET/CT are justified by its unique ability to measure calcification activity specific to the coronary vasculature. Moreover, 18F-NaF is a very simple and relatively cheap ligand to produce.

The majority of our patients had either concomitant aortic stenosis or aortic sclerosis. Although atherosclerosis and aortic stenosis often co-exist and share many common etiological factors and histopathological similarities, it is nevertheless important to confirm these findings in a cohort of patients more representative of the clinical population with atherosclerosis in the absence of aortic stenosis.

Finally, risk prediction scores are intended to predict events in asymptomatic patients and therefore are not strictly applicable to subjects with an established clinical diagnosis of ischemic heart disease or aortic valve disease. Given these issues, we acknowledge that our data with respect to risk prediction are preliminary and need validation in further prospective clinical trials. However, these scores remained higher in patients with increased coronary NaF uptake even after patients with prior MACE were excluded from the analysis. Therefore we believe that this approach has helped to establish an association between 18F-NaF activity and the presence of traditional cardiovascular risk factors and provides a potential assessment of the risk of future cardiovascular events.

Conclusions

18F-NaF holds promise as a noninvasive method for investigating the role of active calcification in coronary atherosclerosis. There was a strong correlation with established coronary calcium, but 41% of patients with calcium scores >1,000 had no significant 18F-NaF uptake. This suggests that 18F-NaF uptake provides different information, relating to metabolically active calcific plaque and developing micro-calcification. Moreover, this information seems to be of clinical significance in relation to symptomatic status, prior MACE events, and cardiovascular risk scores. Prospective studies to determine the relationship between 18F-NaF uptake, morphological plaque characteristics, and future cardiovascular events are now needed in subjects with stable and unstable CAD.

Acknowledgments

The authors are grateful to the Wellcome Trust Clinical Research Facility and the Clinical Research Imaging Centre for their help with this study.

Reprint requests and correspondence: Dr. Marc Dweck, Centre for Cardiovascular Science, University of Edinburgh, Little France Crescent, Edinburgh EH16 4TJ, United Kingdom. E-mail: MDweck@staffmail.ed.ac.uk.

REFERENCES

1. Roger VL, Go AS, Lloyd-Jones DM, et al. Heart disease and stroke statistics—2011 update: a report from the American Heart Association. Circulation 2011;123:e18–209.
2. Gaziano TA. Cardiovascular disease in the developing world and its cost-effective management. Circulation 2005;112:3547–53.
3. Davies MJ. The pathophysiology of acute coronary syndromes. Heart 2000;83:361–6.
4. Kolodgie FD, Burke AP, Farb A, et al. The thin-cap fibroatheroma: a type of vulnerable plaque: the major precursor lesion to acute coronary syndromes. Curr Opin Cardiol 2001;16:285–92.
5. Budoff MJ, Gul KM. Expert review on coronary calcium. Vasc Health Risk Manag 2008;4:315–24.
6. Raggi P, Callister TQ, Shaw LJ. Progression of coronary artery calcium and risk of first myocardial infarction in patients receiving cholesterol-lowering therapy. Arterioscler Thromb Vasc Biol 2004;24:1272–7.

7. McEvoy JW, Blaha MJ, Defilippis AP, et al. Coronary artery calcium progression: an important clinical measurement? A review of published reports. J Am Coll Cardiol; 56:1613–22.
8. Motoyama S, Kondo T, Sarai M, et al. Multislice computed tomographic characteristics of coronary lesions in acute coronary syndromes. J Am Coll Cardiol 2007;50:319–26.
9. Huang H, Virmani R, Younis H, Burke AP, Kamm RD, Lee RT. The impact of calcification on the biomechanical stability of atherosclerotic plaques. Circulation 2001;103:1051–6.
10. Ehara S, Kobayashi Y, Yoshiyama M, et al. Spotty calcification typifies the culprit plaque in patients with acute myocardial infarction: an intravascular ultrasound study. Circulation 2004;110:3424–9.
11. Vengrenyuk Y, Carlier S, Xanthos S, et al. A hypothesis for vulnerable plaque rupture due to stress-induced debonding around cellular microcalcifications in thin fibrous caps. Proc Natl Acad Sci U S A 2006;103:14678–83.
12. Even-Sapir E, Metser U, Mishani E, Lievshitz G, Lerman H, Leibovitch I. The detection of bone metastases in patients with high-risk prostate cancer: 99mTc-MDP Planar bone scintigraphy, single- and multi-field-of-view SPECT, 18F-fluoride PET, and 18F-fluoride PET/CT. J Nucl Med 2006;47:287–97.
13. Derlin T, Toth Z, Papp L, et al. Correlation of inflammation assessed by 18F-FDG PET, active mineral deposition assessed by 18F-fluoride PET, and vascular calcification in atherosclerotic plaque: a dual-tracer PET/CT study. J Nucl Med 2011;52:1020–7.
14. Derlin T, Richter U, Bannas P, et al. Feasibility of 18F-sodium fluoride PET/CT for imaging of atherosclerotic plaque. J Nucl Med 2010;51:862–5.
15. Derlin T, Wisotzki C, Richter U, et al. In vivo imaging of mineral deposition in carotid plaque using 18F-sodium fluoride PET/CT: correlation with atherogenic risk factors. J Nucl Med 2011;52:362–8.
16. Libby P. The molecular mechanisms of the thrombotic complications of atherosclerosis. J Intern Med 2008;263:517–27.
17. Rudd JH, Narula J, Strauss HW, et al. Imaging atherosclerotic plaque inflammation by fluorodeoxyglucose with positron emission tomography: ready for prime time? J Am Coll Cardiol 2010;55:2527–35.
18. Tawakol A, Migrino RQ, Bashian GG, et al. In vivo 18F-fluorodeoxyglucose positron emission tomography imaging provides a noninvasive measure of carotid plaque inflammation in patients. J Am Coll Cardiol 2006;48:1818–24.
19. Rudd JH, Warburton EA, Fryer TD, et al. Imaging atherosclerotic plaque inflammation with [18F]-fluorodeoxyglucose positron emission tomography. Circulation 2002;105:2708–11.
20. Kim TN, Kim S, Yang SJ, et al. Vascular inflammation in patients with impaired glucose tolerance and type 2 diabetes: analysis with 18F-fluorodeoxyglucose positron emission tomography. Circ Cardiovasc Imaging 2010;3:142–8.
21. Tahara N, Kai H, Ishibashi M, et al. Simvastatin attenuates plaque inflammation: evaluation by fluorodeoxyglucose positron emission tomography. J Am Coll Cardiol 2006;48:1825–31.
22. Fayad ZA, Mani V, Woodward M, et al. Safety and efficacy of dalcetrapib on atherosclerotic disease using novel non-invasive multimodality imaging (dal-PLAQUE): a randomised clinical trial. Lancet 2011;378:1547–59.
23. Folco EJ, Sheikine Y, Rocha VZ, et al. Hypoxia but not inflammation augments glucose uptake in human macrophages implications for imaging atherosclerosis with (18)fluorine-labeled 2-deoxy-d-glucose positron emission tomography. J Am Coll Cardiol 2011;58:603–14.
24. Rogers IS, Nasir K, Figueroa AL, et al. Feasibility of FDG imaging of the coronary arteries: comparison between acute coronary syndrome and stable angina. J Am Coll Cardiol Img 2010;3:388–97.
25. Izquierdo-Garcia D, Davies JR, Graves MJ, et al. Comparison of methods for magnetic resonance-guided [18-F]fluorodeoxyglucose positron emission tomography in human carotid arteries: reproducibility, partial volume correction, and correlation between methods. Stroke 2009;40:86–93.
26. Dweck MR, Jones C, Joshi N, et al. Assessment of valvular calcification and inflammation by positron emission tomography in patients with aortic stenosis. Circulation 2012;125:76–86.
27. Wykrzykowska J, Lehman S, Williams G, et al. Imaging of inflamed and vulnerable plaque in coronary arteries with 18F-FDG PET/CT in patients with suppression of myocardial uptake using a low-carbohydrate, high-fat preparation. J Nucl Med 2009;50:563–8.
28. Williams G, Kolodny GM. Suppression of myocardial 18F-FDG uptake by preparing patients with a high-fat, low-carbohydrate diet. AJR Am J Roentgenol 2008;190:W151–6.
29. Cheng VY, Slomka PJ, Ahlen M, Thomson LE, Waxman AD, Berman DS. Impact of carbohydrate restriction with and without fatty acid loading on myocardial (18)F-FDG uptake during PET: a randomized controlled trial. J Nucl Cardiol 2010;17:286–91.
30. Agatston AS, Janowitz WR, Hildner FJ, Zusmer NR, Viamonte M Jr., Detrano R. Quantification of coronary artery calcium using ultrafast computed tomography. J Am Coll Cardiol 1990;15:827–32.
31. Rudd JH, Myers KS, Bansilal S, et al. Atherosclerosis inflammation imaging with 18F-FDG PET: carotid, iliac, and femoral uptake reproducibility, quantification methods, and recommendations. J Nucl Med 2008;49:871–8.
32. Rudd JH, Myers KS, Bansilal S, et al. Relationships among regional arterial inflammation, calcification, risk factors, and biomarkers: a prospective fluorodeoxyglucose positron-emission tomography/computed tomography imaging study. Circ Cardiovasc Imaging 2009;2:107–15.
33. Taylor AJ, Cerqueira M, Hodgson JM, et al. ACCF/SCCT/ACR/AHA/ASE/ASNC/NASCI/SCAI/SCMR 2010 appropriate use criteria for cardiac computed tomography. A report of the American College of Cardiology Foundation Appropriate Use Criteria Task Force, the Society of Cardiovascular Computed Tomography, the American College of Radiology, the American Heart Association, the American Society of Echocardiography, the American Society of Nuclear Cardiology, the North American Society for Cardiovascular Imaging, the Society for Cardiovascular Angiography and Interventions, and the Society for Cardiovascular Magnetic Resonance. J Am Coll Cardiol 2010;56:1864–94.
34. Weber WA, Ziegler SI, Thodtmann R, Hanauske AR, Schwaiger M. Reproducibility of metabolic measurements in malignant tumors using FDG PET. J Nucl Med 1999;40:1771–7.
35. Blau M, Ganatra R, Bender MA. 18 F-fluoride for bone imaging. Semin Nucl Med 1972;2:31–7.
36. Installe J, Nzeusseu A, Bol A, Depresseux G, Devogelaer JP, Lonneux M. (18)F-fluoride PET for monitoring therapeutic response in Paget's disease of bone. J Nucl Med 2005;46:1650–8.
37. Grant FD, Fahey FH, Packard AB, Davis RT, Alavi A, Treves ST. Skeletal PET with 18F-fluoride: applying new technology to an old tracer. J Nucl Med 2008;49:68–78.
38. Virmani R, Burke AP, Farb A, Kolodgie FD. Pathology of the vulnerable plaque. J Am Coll Cardiol 2006;47:C13–8.
39. Burke AP, Weber DK, Kolodgie FD, Farb A, Taylor AJ, Virmani R. Pathophysiology of calcium deposition in coronary arteries. Herz 2001;26:239–44.
40. Stary HC, Chandler AB, Dinsmore RE, et al. A definition of advanced types of atherosclerotic lesions and a histological classification of atherosclerosis. A report from the Committee on Vascular Lesions of the Council on Arteriosclerosis, American Heart Association. Arterioscler Thromb Vasc Biol 1995;15:1512–31.
41. Ueda M. [Clinical relevance of coronary artery calcification, as a risk factor for plaque rupture: viewpoint from pathology]. Clin Calcium; 20:1656–62.
42. de Feyter PJ, Ozaki Y, Baptista J, et al. Ischemia-related lesion characteristics in patients with stable or unstable angina. A study with intracoronary angioscopy and ultrasound. Circulation 1995;92:1408–13.
43. Thieme T, Wernecke KD, Meyer R, et al. Angioscopic evaluation of atherosclerotic plaques: validation by histomorphologic analysis and association with stable and unstable coronary syndromes. J Am Coll Cardiol 1996;28:1–6.
44. Wu X, Maehara A, Mintz GS, et al. Virtual histology intravascular ultrasound analysis of non-culprit attenuated plaques detected by grayscale intravascular ultrasound in patients with acute coronary syndromes. Am J Cardiol 2010;105:48–53.

Key Words: acute coronary syndrome ■ calcification ■ inflammation ■ positron emission tomography ■ risk prediction.

APPENDIX

For a supplemental video, please see the online version of this article.